# Germylene Energetics: Electron Affinities and Singlet−Triplet Gaps of $GeX_2$ and GeXY Species (X, Y = H, $CH_3$, $SiH_3$, $GeH_3$, F, Cl, Br, I)

**Ashwini Bundhun,[†] Ponnadurai Ramasami,*[,†] and Henry F. Schaefer III*[,‡]**

*Department of Chemistry, University of Mauritius, Réduit, Mauritius, and Center for Computational Quantum Chemistry, University of Georgia, Athens, Georgia 30602*

*Received: January 25, 2009; Revised Manuscript Received: May 21, 2009*

A systematic investigation of the $GeX_2$ and GeXY species was carried out using the popular DFT functionals BLYP, B3LYP, and BHHLYP. Predicted are the singlet−triplet energy gaps and four types of neutral−anion separations: adiabatic electron affinity ($EA_{ad}$), zero-point vibrational energy corrected $EA_{ad(ZPVE)}$, vertical electron affinity ($EA_{vert}$), and vertical detachment energy. The basis sets used for all atoms in this work are of double-$\zeta$ plus polarization quality with additional s- and p-type diffuse functions denoted DZP++, except for iodine where the 6-311G(d,p) basis set is used. The geometries are fully optimized with each functional independently. Vibrational frequency analyses were performed to compute zero-point energy corrections and to determine the nature of the stationary points. The geometries and the relative energies are discussed and compared with the carbon and silicon analogues. The $EA_{ad(ZPVE)}$ values (eV) obtained with the B3LYP functional range from 0.62 eV [$Ge(CH_3)_2$] to 2.08 eV [$Ge(GeH_3)_2$]. These results compare satisfactorily with the few available experiments, but most are reported for the first time. Similarly, the predicted singlet−triplet energy separations range from 13.8 kcal $mol^{-1}$ [$Ge(SiH_3)_2$] to 85.0 kcal $mol^{-1}$ [$GeF_2$]. Invariably, as one progresses down the periodic table C → Si → Ge, the "great divide" occurs between carbon and silicon.

## I. Introduction

Germylenes, divalent germanium compounds[1−4] $GeR_2$, have evolved over the past 20 years from exotic reaction intermediates to important chemical species.[5−12] The progress in this field over the past 5 years is particularly impressive.[13−32] A spectacular, very recent example is the use of germylene methodology to synthesize an encapsulated germanium(II) dication.[33] Moreover, the increasing importance of plasma etching and deposition processes[34] plays a significant role in the production of high-performance microelectronics products and thus has necessitated detailed knowledge of the species involved in these processes. The geometrical properties of germanium-related compounds have attracted much interest, since these are considered to be intermediates in many of the processes employed in the semiconductor industry.[35]

Since only few gas-phase germanium-containing species have been studied experimentally and theoretically, the present research aims at providing electronic properties for the structures $GeX_2$ and GeXY, where reliable experimental data is scarce. Balasubramanian[36,37] have studied the geometry of the $^1A_1$ ground state of $GeH_2$ at the CASSCF/SOCI levels of theory and multireference singles and doubles CI (MRSDCI) and reported $r_e$(Ge−H) = 1.587 Å, $\theta_e$(H−Ge−H) = 91.5°, and singlet−triplet energy separation of 23 kcal $mol^{-1}$. Recently this has been reproduced theoretically by Li et al.[38] by using carefully calibrated DZP++ basis sets found to be consistent with previous experiments on other systems. Moreover, the energy differences provided by Li et al.,[38] ranging from 1.03 eV (BHLYP) to 1.18 eV (B3LYP), showed good agreement with the experimental value.[39] Ito, Hirota, and Kuchitsu[40,41] have provided valuable experimental information on the spectroscopic properties of GeHCl and GeHBr using the laser-induced fluorescence (LIF) techniques.

Balasubramanian et al.[42,43] have also predicted the equilibrium geometries and the energy separations of the low-lying electronic states of $GeF_2$, $GeCl_2$, $GeBr_2$ and $GeI_2$, GeHCl, GeHBr, and GeHI using the complete-active-space multiconfiguration self-consistent field (CAS-MCSCF) method followed by multireference configuration interaction (MRCI). Takeo et al.[44] deduced the experimental structure ($r_e$ = 1.732 Å and $\theta_e$ = 97.1°) from the microwave spectrum of $GeF_2$. These results were further compared with Balasubramanian's CAS-MCSCF and MRSDCI-(+Q) results. In 1977, Pabst et al.[45] carried out electron impact studies for $GeCl_2$ and $GeBr_2$, and the electron affinities were reported to be 2.56 and > 1.6 eV, respectively. In view of the concluding remarks made by Li et al.[38] that the three functionals B3LYP, BHLYP, and BLYP gave reasonable results for the electron affinities, these results have provided considerable motivation for benchmarking the current research work in predicting the abilities of germylenes to bind an extra electron. Sherrill et al.[46] have benchmarked full configuration interaction methods representing the exact solution of the electronic Schrödinger equation for four lowest lying electronic states of methylene ($^3B_1$, $^1A_1$, $^1B_1$) with the DZP basis set. They reported full CI energies, equilibrium geometrical parameters, dipole moments, harmonic vibrational frequencies, and the singlet−triplet energy gap. Later computed BLYP/DZP++ singlet−triplet splittings for the silicon analogue,[47] $SiH_2$, resulted in a singlet−triplet energy separation of 20.0 kcal $mol^{-1}$.

## II. Theoretical Methods

Geometrical parameters, adiabatic electron affinities, ZPVE-corrected electron affinities, vertical electron affinities, and vertical detachment energies of the anions and singlet−triplet

* Authors for correspondence: P.R., ramchemi@intnet.mu; H.F.S., sch@uga.edu.
[†] Department of Chemistry, University of Mauritius.
[‡] Center for Computational Quantum Chemistry, University of Georgia.

10.1021/jp900735w CCC: $40.75 
Published on Web 06/23/2009

gaps have been computed with the Gaussian 03 program.[48] Three different density functionals, namely, BHLYP, B3LYP, and BLYP, were used. BHLYP is an HF/DFT hybrid method comprising the Becke (B)[49] half and half exchange functional (H)[50] along with the Lee, Yang, and Parr (LYP)[51] nonlocal correlation functional. The B3LYP method is also an HF/DFT hybrid method using the B3 exchange along with the LYP correlation functional. The BLYP method is a pure DFT method, comprised of the B exchange functional along with the LYP correlation. All structures are independently optimized with each of the three functionals.

The double-ζ basis sets with polarization and diffuse functions, denoted as DZP++, are used for all atoms except for iodine atom, where the 6-311G(d,p) basis set is used. The double-ζ basis sets were constructed by augmenting the Huzinaga−Dunning−Hay[52−54] sets of contracted Gaussian functions with one set of p polarization functions for each H atom and one set of d polarization functions for each heavy atom, respectively ($\alpha_p(H) = 0.75$, $\alpha_d(C) = 0.75$, $\alpha_d(F) = 1.0$, $\alpha_d(Si) = 0.5$, $\alpha_d(Cl) = 0.75$, $\alpha_d(Br) = 0.389$). The above basis sets were further augmented with diffuse functions, where each atom received one additional s-type and one additional set of p-type functions. Each H atom basis set is appended with one diffuse s-function. The diffuse functions were determined in an even-tempered fashion following the prescription of Lee[55]

$$\alpha_{\text{diffuse}} = \frac{1}{2}\left(\frac{\alpha_1}{\alpha_2} + \frac{\alpha_2}{\alpha_3}\right)\alpha_1$$

where $\alpha_1$, $\alpha_2$, and $\alpha_3$ are the three smallest Gaussian orbital exponents of the s- or p-type primitive functions of a given atom ($\alpha_1 < \alpha_2 < \alpha_3$). Thus $\alpha_s(H) = 0.04415$, $\alpha_s(C) = 0.04302$, $\alpha_p(C) = 0.03629$, $\alpha_s(F) = 0.1049$, $\alpha_p(F) = 0.0826$, $\alpha_s(Si) = 0.02729$, $\alpha_p(Si) = 0.025$, $\alpha_s(Cl) = 0.05048$, $\alpha_p(Cl) = 0.05087$, $\alpha_s(Br) = 0.0469096$, and $\alpha_p(Br) = 0.0465342$.

The DZP++ basis set for germanium was comprised of the Schafer−Horn−Ahlrichs double-ζ spd set plus a set of five pure d-type polarization functions with $\alpha_d(Ge) = 0.246$ augmented by a set of sp diffuse functions with $\alpha_s(Ge) = 0.024434$ and $\alpha_p(Ge) = 0.023059$.[56] The overall contraction scheme for the basis sets is H(5s1p/3s1p), C(10s6p1d/5s3p1d), F(10s6p1d/5s3p1d), Si(13s9p1d/7s5p1d), Cl(13s9p1d/7s5p1d), Ge(15s12p6d/9s7p3d), and Br(15s12p6d/9s7p3d). In all cases an extended integration grid (199,974) was applied. The four forms of the neutral−anion energy difference are evaluated by the following scheme.

The adiabatic electron affinities are determined by: (i) $EA_{ad}$ = *E*(optimized neutral) − *E*(optimized anion).

Vertical electron affinity is determined by (ii) $EA_{vert}$ = *E*(optimized neutral) − *E*(anion at optimized neutral geometry.

The vertical detachment energy of the anion is determined by (iii) VDE = *E*(neutral at optimized anion geometry) − *E*(optimized anion).

Additionally, zero-point vibrational energies (ZPVE) were evaluated at each level. The corrected adiabatic electron affinities $EA_{ad(ZPVE)}$ between the neutral and the anionic species are reported as follows: (iv) $EA_{ad(ZPVE)} = [E(\text{optimized neutral}) + ZPVE_{neutral}] - [E(\text{optimized anion}) + ZPVE_{anion}]$.

Finally, the singlet−triplet splittings are predicted as the energy differences between the neutral ground state and the lowest triplet state.

**TABLE 1: Germylene Adiabatic Electron Affinities $EA_{ad}$ and Zero-Point Corrected $EA_{ad}$ Values (in parentheses) in Electronvolts[a]**

| | BH & HLYP | BLYP | B3LYP | $SiR_2$ BH & HLYP |
|---|---|---|---|---|
| **Ge**$H_2$[b] | 1.01 (1.03) | 1.02 (1.05) | 1.15 (1.18) | 1.02 |
| **Ge**$F_2$ | 0.85 (0.87) | 0.81 (0.83) | 0.96 (0.98) | 0.41 |
| **Ge**$Cl_2$ | 1.65 (1.66) | 1.49 (1.50) | 1.69 (1.70) | 1.50 |
| **Ge**$Br_2$ | 1.81 (1.82) | 1.60 (1.61) | 1.83 (1.84) | 1.72 |
| **Ge**$I_2$ | 2.06 (2.07) | 1.76 (1.77) | 2.03 (2.04) | |
| **Ge**HF | 0.96 (0.98) | 0.94 (0.96) | 1.08 (1.10) | 0.76 |
| **Ge**HCl | 1.36 (1.39) | 1.28 (1.30) | 1.45 (1.47) | 1.29 |
| **Ge**HBr | 1.45 (1.47) | 1.34 (1.36) | 1.53 (1.55) | 1.41 |
| **Ge**HI | 1.59 (1.61) | 1.42 (1.44) | 1.63 (1.65) | |
| **Ge**FCl | 1.28 (1.30) | 1.17 (1.19) | 1.35 (1.37) | 0.99 |
| **Ge**FBr | 1.38 (1.40) | 1.25 (1.27) | 1.44 (1.46) | 1.14 |
| **Ge**FI | 1.55 (1.56) | 1.35 (1.37) | 1.57 (1.59) | |
| **Ge**ClBr | 1.73 (1.75) | 1.55 (1.56) | 1.76 (1.77) | 1.61 |
| **Ge**ClI | 1.87 (1.88) | 1.63 (1.64) | 1.87 (1.88) | |
| **Ge**BrI | 1.94 (1.95) | 1.68 (1.69) | 1.93 (1.94) | |
| H**Ge**$CH_3$ | 0.69 (0.71) | 0.72 (0.75) | 0.84 (0.86) | 0.65 |
| F**Ge**$CH_3$ | 0.64 (0.66) | 0.65 (0.67) | 0.77 (0.79) | 0.40 |
| Cl**Ge**$CH_3$ | 1.07 (1.09) | 1.01 (1.03) | 1.17 (1.18) | 1.03 |
| Br**Ge**$CH_3$ | 1.17 (1.19) | 1.09 (1.10) | 1.26 (1.27) | 1.09 |
| I**Ge**$CH_3$ | 1.33 (1.33) | 1.19 (1.20) | 1.39 (1.40) | |
| H**Ge**$SiH_3$ | 1.48 (1.51) | 1.47 (1.50) | 1.62 (1.65) | |
| H**Ge**$GeH_3$[b] | 1.51 (1.55) | 1.52 (1.55) | 1.65 (1.69) | 1.55 |
| F**Ge**$SiH_3$ | 1.44 (1.47) | 1.39 (1.45) | 1.55 (1.58) | |
| F**Ge**$GeH_3$ | 1.47 (1.50) | 1.44 (1.48) | 1.59 (1.62) | 1.31 |
| Cl**Ge**$SiH_3$ | 1.78 (1.80) | 1.68 (1.70) | 1.86 (1.88) | |
| Cl**Ge**$GeH_3$ | 1.80 (1.83) | 1.71 (1.72) | 1.89 (1.92) | 1.77 |
| Br**Ge**$SiH_3$ | 1.85 (1.87) | 1.73 (1.75) | 1.92 (1.94) | |
| Br**Ge**$GeH_3$ | 1.87 (1.89) | 1.76 (1.78) | 1.94 (1.97) | 1.86 |
| I**Ge**$SiH_3$ | 1.97 (1.98) | 1.80 (1.81) | 2.01 (2.03) | |
| I**Ge**$GeH_3$ | 1.98 (2.00) | 1.82 (1.85) | 2.03 (2.05) | |
| $CH_3$**Ge**$SiH_3$ | 1.20 (1.22) | 1.20 (1.23) | 1.34 (1.37) | |
| $CH_3$**Ge**$GeH_3$ | 1.23 (1.26) | 1.25 (1.29) | 1.38 (1.41) | 1.23 |
| **Ge**$(CH_3)_2$ | 0.44 (0.46) | 0.49 (0.52) | 0.60 (0.62) | 0.38 |
| **Ge**$(SiH_3)_2$ | 1.87 (1.90) | 1.83 (1.86) | 1.99 (2.06) | |
| **Ge**$(GeH_3)_2$ | 1.91 (1.95) | 1.89 (1.93) | 2.04 (2.08) | 1.98 |

[a] The boldface **Ge** designates the divalent germanium atom. The last column reports analogous results for silylene derivatives, from ref 47. [b] Reference 38.

## III. Results

This section is composed of the results obtained in the present research and includes a comparison with reported literature findings for the germanium-containing species only.

**A. $GeH_2$ and $GeH_2^-$.** The optimized geometries of Li et al.[38] for the neutral ground state $^1A_1$ $GeH_2$ show the bond length Ge−H to range from 1.584 Å (BHLYP) to 1.617 Å (BLYP), while the predicted H−Ge−H bond angle goes from 90.3° (BLYP) to 91.5° (BHLYP). The corresponding $^2B_1$ ground state anion $GeH_2^-$ had predicted bond lengths of 1.629, 1.647, and 1.612 Å and bond angles of 91.5°, 91.2°, and 92.2° (B3LYP, BLYP, BHLYP), respectively. The electron affinities for $GeH_2$ species[38] are included in Tables 1−3 for comparison purposes. These computed electron affinities are in agreement with the experimental value reported in literature as 1.097 eV.[39] The optimized geometry of the lowest triplet state $^3B_1$ $GeH_2$ is seen in Figure 1. The Ge−H bond length decreases by 0.051 Å, with a marked increase in the bond angle by 28.1° with respect to the $^1A_1$ neutral ground state $GeH_2$. The singlet−triplet splittings for $GeH_2$ range from 1.06 eV (BHLYP) to 1.23 eV (BLYP).

**B. $Ge(CH_3)_2$ and $Ge(CH_3)_2^-$.** The equilibrium geometries of the $^1A$ ground state $Ge(CH_3)_2$ ($C_1$ symmetry), the ground state anion $^2A'$ $Ge(CH_3)_2^-$ ($C_s$ symmetry), and the $^3A$ triplet state of $Ge(CH_3)_2$ ($C_1$ symmetry) are presented in Figure 2.

**TABLE 2: Vertical Electron Affinities (VEA) in Electronvolts**

| | BH & HLYP | BLYP | B3LYP |
|---|---|---|---|
| **Ge**$H_2$[a] | 0.99 | 1.01 | 1.14 |
| **Ge**$F_2$ | 0.69 | 0.67 | 0.81 |
| **Ge**$Cl_2$ | 1.38 | 1.25 | 1.44 |
| **Ge**$Br_2$ | 1.56 | 1.39 | 1.60 |
| **Ge**$I_2$ | 1.84 | 1.58 | 1.83 |
| **Ge**HF | 0.87 | 0.86 | 0.99 |
| **Ge**HCl | 1.20 | 1.13 | 1.30 |
| **Ge**HBr | 1.29 | 1.20 | 1.37 |
| **Ge**HI | 1.43 | 1.28 | 1.49 |
| **Ge**FCl | 1.05 | 0.97 | 1.13 |
| **Ge**FBr | 1.15 | 1.05 | 1.22 |
| **Ge**FI | 1.32 | 1.16 | 1.37 |
| **Ge**ClBr | 1.47 | 1.32 | 1.52 |
| **Ge**ClI | 1.63 | 1.63 | 1.65 |
| **Ge**BrI | 1.70 | 1.49 | 1.72 |
| H**Ge**$CH_3$ | 0.64 | 0.67 | 0.79 |
| F**Ge**$CH_3$ | 0.53 | 0.55 | 0.67 |
| Cl**Ge**$CH_3$ | 0.89 | 0.85 | 1.00 |
| Br**Ge**$CH_3$ | 1.00 | 0.93 | 1.09 |
| I**Ge**$CH_3$ | 1.16 | 1.04 | 1.23 |
| H**Ge**$SiH_3$ | 1.38 | 1.37 | 1.52 |
| H**Ge**$GeH_3$[a] | 1.41 | 1.42 | 1.55 |
| F**Ge**$SiH_3$ | 1.28 | 1.25 | 1.40 |
| F**Ge**$GeH_3$ | 1.31 | 1.29 | 1.43 |
| **Cl****Ge**$SiH_3$ | 1.57 | 1.49 | 1.67 |
| Cl**Ge**$GeH_3$ | 1.59 | 1.53 | 1.69 |
| Br**Ge**$SiH_3$ | 1.64 | 1.55 | 1.73 |
| Br**Ge**$GeH_3$ | 1.66 | 1.58 | 1.75 |
| I**Ge**$SiH_3$ | 1.77 | 1.63 | 1.83 |
| I**Ge**$GeH_3$ | 1.79 | 1.66 | 1.85 |
| $CH_3$**Ge**$SiH_3$ | 1.06 | 1.05 | 1.19 |
| $CH_3$**Ge**$GeH_3$ | 1.10 | 1.11 | 1.24 |
| **Ge**$(CH_3)_2$ | 0.35 | 0.36 | 0.51 |
| **Ge**$(SiH_3)_2$ | 1.66 | 1.61 | 1.78 |
| **Ge**$(GeH_3)_2$ | 1.72 | 1.70 | 1.84 |

[a] Reference 38.

**TABLE 3: Vertical Detachment Energies (VDE) in Electronvolts**

| | BH & HLYP | BLYP | B3LYP |
|---|---|---|---|
| **Ge**$H_2$[a] | 1.02 | 1.03 | 1.16 |
| **Ge**$F_2$ | 1.04 | 0.98 | 1.14 |
| **Ge**$Cl_2$ | 1.97 | 1.76 | 1.99 |
| **Ge**$Br_2$ | 2.11 | 1.86 | 2.10 |
| **Ge**$I_2$ | 2.32 | 1.97 | 2.26 |
| **Ge**HF | 1.06 | 1.03 | 1.18 |
| **Ge**HCl | 1.57 | 1.45 | 1.64 |
| **Ge**HBr | 1.66 | 1.52 | 1.71 |
| **Ge**HI | 1.78 | 1.58 | 1.81 |
| **Ge**FCl | 1.57 | 1.42 | 1.62 |
| **Ge**FBr | 1.68 | 1.50 | 1.71 |
| **Ge**FI | 1.83 | 1.59 | 1.83 |
| **Ge**ClBr | 2.05 | 1.81 | 2.05 |
| **Ge**ClI | 2.17 | 1.88 | 2.14 |
| **Ge**BrI | 2.22 | 1.92 | 2.19 |
| H**Ge**$CH_3$ | 0.74 | 0.77 | 0.89 |
| F**Ge**$CH_3$ | 0.77 | 0.76 | 0.89 |
| Cl**Ge**$CH_3$ | 1.29 | 1.19 | 1.37 |
| Br**Ge**$CH_3$ | 1.40 | 1.27 | 1.46 |
| I**Ge**$CH_3$ | 1.55 | 1.37 | 1.58 |
| H**Ge**$SiH_3$ | 1.59 | 1.56 | 1.72 |
| H**Ge**$GeH_3$[a] | 1.62 | 1.61 | 1.76 |
| F**Ge**$SiH_3$ | 1.61 | 1.55 | 1.72 |
| F**Ge**$GeH_3$ | 1.64 | 1.60 | 1.76 |
| Cl**Ge**$SiH_3$ | 2.02 | 1.88 | 2.08 |
| Cl**Ge**$GeH_3$ | 2.03 | 1.92 | 2.10 |
| Br**Ge**$SiH_3$ | 2.08 | 1.93 | 2.13 |
| Br**Ge**$GeH_3$ | 2.10 | 1.96 | 2.16 |
| I**Ge**$SiH_3$ | 2.19 | 1.98 | 2.21 |
| I**Ge**$GeH_3$ | 2.20 | 2.01 | 2.23 |
| $CH_3$**Ge**$SiH_3$ | 1.32 | 1.31 | 1.45 |
| $CH_3$**Ge**$GeH_3$ | 1.35 | 1.36 | 1.49 |
| **Ge**$(CH_3)_2$ | 0.50 | 0.53 | 0.66 |
| **Ge**$(SiH_3)_2$ | 2.04 | 1.99 | 2.19 |
| **Ge**$(GeH_3)_2$ | 2.08 | 2.05 | 2.20 |

[a] Reference 38.

There is an increase in the Ge−C bond distance of 0.065 Å from the neutral to the anion with a concomitant decrease in bond angle by 2.1°. The $EA_{ad(ZPVE)}$ values range from 0.46 to 0.62 eV, with BHLYP and B3LYP as the lower and upper bounds, respectively. The $EA_{(vert)}$ is small, ranging from 0.35 eV (BHLYP) to 0.51 eV (B3LYP), and the VDE is slightly larger ranging from 0.50 to 0.66 eV. The singlet−triplet splittings for $Ge(CH_3)_2$ increase from 1.26 to 1.38 eV in the order BHLYP < B3LYP < BLYP. As seen from Table 1, the inductive effect of the presence of the two $CH_3$ moieties in $Ge(CH_3)_2$ is even more pronounced. The electron-donor ability of the methyl groups causes the electron density near the central germanium to increase. Hence $Ge(CH_3)_2$ has the lowest predicted $EA_{ad(ZPVE)}$, though it can weakly bind an extra electron.

**C. $Ge(GeH_3)_2$ and $Ge(GeH_3)_2^-$.** Figure 3 presents the optimized geometrical parameters for the $^1A$ ground state $Ge(GeH_3)_2$, the $^2A$ state of the $Ge(GeH_3)_2^-$ anion, and the $^3B_1$ triplet state of $Ge(GeH_3)_2$. The addition of an extra electron reveals an increase in the Ge−Ge bond lengths by 0.007 Å, with a corresponding increase in the Ge−Ge−Ge bond angle by 0.3°, as well as an increase in the Ge−H bond distances of 0.026 Å. The Ge−Ge bond lengths of the $^3B_1$ triplet state of $Ge(GeH_3)_2$ decrease by 0.059 Å from those for the $^1A$ ground state $Ge(GeH_3)_2$. There is an appreciable $^3B_1-{}^1A_1$ increase in the Ge−Ge−Ge bond angle of 31.9°, together with a slight decrease in the Ge−H bond length of 0.006 Å. One observes a dramatic *increase* in the electron affinities on substitution of $GeH_3$ groups, but an even greater increase upon comparison with $HGeCH_3$, by nearly 0.80 eV (BHLYP). The $GeH_3$ substituents increase the $EA_{ad(ZPVE)}$ by 0.92 eV, the VEA by 0.73 eV, and the VDE by 1.06 eV compared to $GeH_2$.

**$GeH_2$ Triplet ($^3B_1$)**

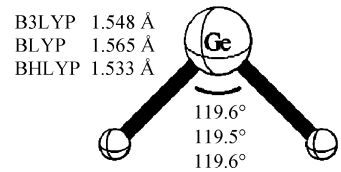


**Figure 1.** Equilibrium geometries for the $^3B_1$ state of $GeH_2$.

**D. $XGeSiH_3$ (X = H, F, Cl, Br, I, $CH_3$), Their Anions and Triplet States.** Only slight increases in the Ge−X bond lengths and bond angles, accompanying a slight decrease in the Ge−Si bond lengths, are observed on addition of an extra electron to the $^1A$ neutral ground state $XGeSiH_3$. The decrease in electron affinities on substitution of the hydrogen atom by a methyl group decreases $EA_{ad(ZPVE)}$ by 0.29 eV, the VEA by 0.32 eV, and the VDE by 0.27 eV. A larger decrease in the electron affinities is observed on substitution by a methyl group as compared to a fluorine atom. There is a larger increase in the electron affinities for the chloro, bromo, and iodo substituents versus the methyl substitutent. All predicted electron affinities and singlet−triplet gaps for $XGeSiH_3$ are found to be lower than their corresponding $XGeGeH_3$ species. The singlet−triplet splitting for $XGeSiH_3$ ranges from 0.73 to 0.91 eV in the order

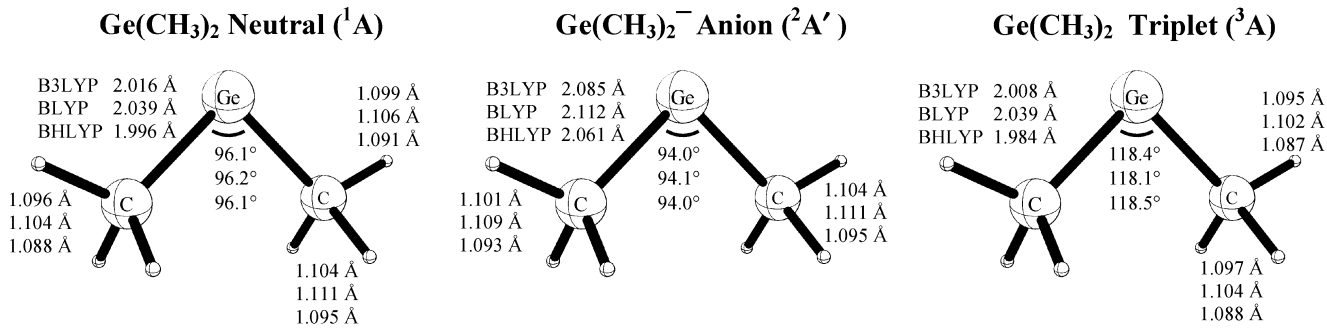


**Figure 2.** Equilibrium geometries for the $^1$A state of $Ge(CH_3)_2$, $^2$A′ state of the $Ge(CH_3)_2^-$ anion, and $^3$A state of the $Ge(CH_3)_2$.

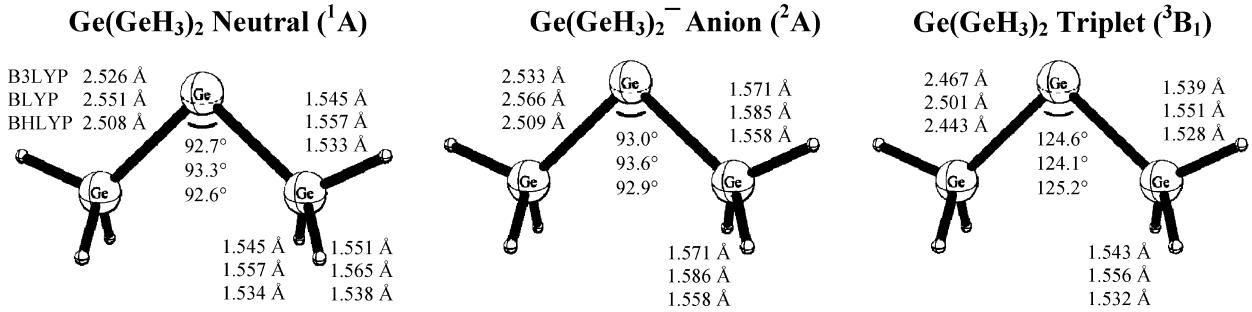


**Figure 3.** Equilibrium geometries for the $^1$A state of $Ge(GeH_3)_2$, $^2$A state of the $Ge(GeH_3)_2^-$ anion, and $^3B_1$ state of the $Ge(GeH_3)_2$.

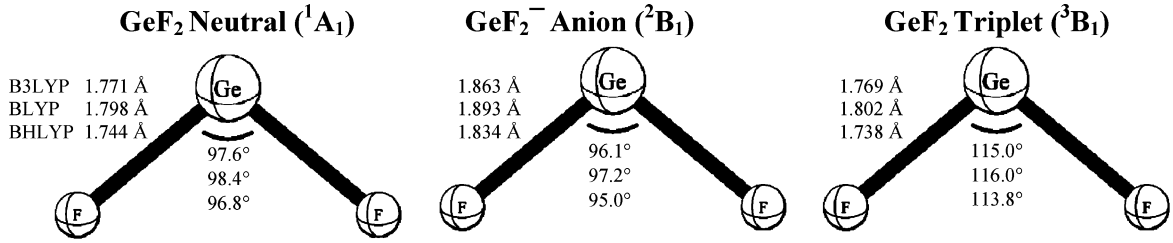


**Figure 4.** Equilibrium geometries for $^1A_1$ state of $GeF_2$, $^2B_1$ state of the $GeF_2^-$ anion, and $^3B_1$ state of $GeF_2$.

BHLYP < B3LYP < BLYP. A larger increase in the singlet−triplet gap is observed for $FGeSiH_3$ relative to the other halogenated systems. Methyl substitution increases the singlet−triplet splitting by only 0.05 eV, with respect to $HGeSiH_3$.

**E. $XGeGeH_3$ (X = H, F, Cl, Br, I, $CH_3$), Their Anions and Triplet States.** In an attempt to assess the effects of halogens and the methyl group for the $XGeGeH_3$ species, all electron affinities are referenced to the neutral $^1$A ground state $HGeGeH_3$ ($C_s$ symmetry) reported by Li et al.[38] Herein, the optimized $^3$A triplet state of $HGeGeH_3$ shows a decrease in the singlet Ge−Ge bond length by 0.076 Å, with a corresponding large increase in the bond angle of 30.4°. Substitution of the hydrogen atom by a methyl group decreases the electron affinity to a much larger extent compared to fluoro substitution, as seen in Table 1. In the case of $CH_3GeGeH_3$, the $EA_{ad(ZPVE)}$ increases by 0.23 eV, the VEA by 0.11 eV, and the VDE by 0.33 eV with respect to $GeH_2$. The addition of a $GeH_3$ group increases the $EA_{ad(ZPVE)}$ by 0.52 eV, the VEA by 0.42 eV, and the VDE by 0.60 eV. There is a marked increase in electron affinities for the chloro, bromo, and iodo substituents versus the methyl and fluoro substituents, which decrease the electron affinities. All optimized geometrical parameters of all species in this set are reported in the Supporting Information.[57]

**F. $GeF_2$ and $GeF_2^-$.** Figure 4 presents the equilibrium geometries of the neutral ground state $^1A_1$ $GeF_2$, $^2B_1$ ground state anion $GeF_2^-$ and the corresponding $^3B_1$ triplet state $GeF_2$. Previous ab initio CASSCF/MRSDCI studies[43] of $^1A_1$ $GeF_2$ predicted a Ge−F bond distance of 1.718 Å and F−Ge−F bond angle of 95.4°, while the $^3B_1$ triplet state $GeF_2$ was predicted to have a Ge−F bond distance of 1.711 Å and bond angle of 112.4°. Balasubramanian's[43] MRSDCI(+Q) studies resulted in a Ge−F bond distance of 1.723 Å and F−Ge−F bond angle of 97.1° for $^1A_1$ $GeF_2$ whereas the triplet state was reported to have a Ge−F bond distance of 1.715 Å and bond angle of 113.1° at the CASSCF level of theory. The BHLYP functional resulted in a $^1A_1$ Ge−F bond distance of 1.744 Å and a bond angle of 96.8°, in closest agreement to the MRSDCI(+Q) level of theory. The singlet−triplet splitting of 3.57 eV obtained with the BHLYP functional is found to be consistent with Balasubramanian's MRSDCI(+Q) result of 3.54 eV which included zero-point corrected energies.

Geometrical changes accompanying the addition of an electron to $GeF_2$ are an increase of 0.03 Å and 0.7° in the bond length and bond angle, respectively. From the neutral to the triplet state, there is a decrease in the bond length of 0.051 Å, while a large increase of 28.1° in the bond angle was predicted. Fluorine has a marked decrease on the $EA_{ad(ZPVE)}$ of germylene, in almost the same manner as that of the methyl substituents, by 0.22 eV. The $GeF_2$ electron affinity after the ZPVE correction, $EA_{ad(ZPVE)}$, falls in the range from 0.83 eV (BLYP) to 0.93 eV (B3LYP). The $GeF_2$ VEA decreases by 0.34 eV compared to $GeH_2$ and the VDE by 0.05 eV. The experimental electron affinity obtained by Harland et al.[58] was >1.30 ± 0.30 eV from the electron impact appearance energy (EIAE). That experiment is in disagreement with the theoretical values

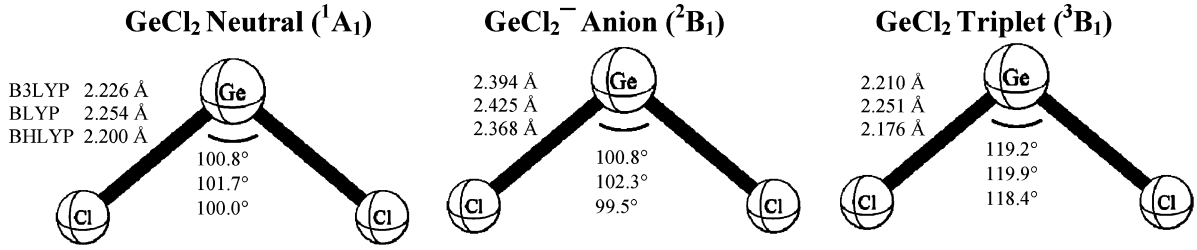


**Figure 5.** Equilibrium geometries of the $^1A_1$ state of $GeCl_2$, $^2B_1$ state of the $GeCl_2^-$ anion, and $^3B_1$ state of $GeCl_2$.

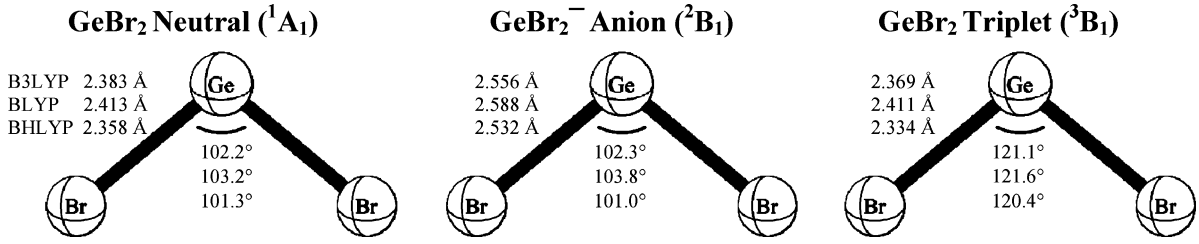


**Figure 6.** Equilibrium geometries of the $^1A_1$ state of $GeBr_2$, $^2B_1$ state of the $GeBr_2^-$ anion, and $^3B_1$ state of $GeBr_2$.

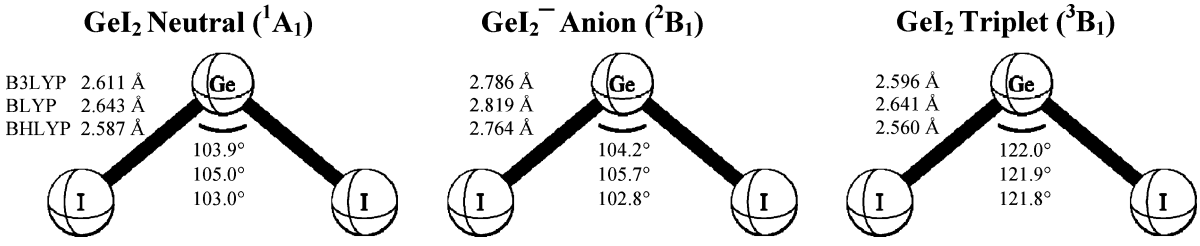


**Figure 7.** Equilibrium geometries of the $^1A_1$ state of $GeI_2$, $^2B_1$ state of the $GeI_2^-$ anion, and $^3B_1$ state of $GeI_2$.

obtained in the present research, which is consistent with the theoretical values obtained by Li et al.[59]

**G. $GeCl_2$ and $GeCl_2^-$.** The equilibrium geometries for the $^1A_1$ state of the neutral $GeCl_2$, the $^2B_1$ state of the anion of $GeCl_2$, and the $^3B_1$ triplet state of $GeCl_2$ are displayed in Figure 5. With respect to the previous results of Balasubramanian,[42] our most reliable bond length and bond angle for $^1A_1$ $GeCl_2$ were found at the B3LYP level. Between the neutral and ground state anion there is a relatively large increase in the bond length of 0.168 Å with a tiny decrease in the bond angle of 0.1°. The differences in the geometrical parameters between the neutral ground state and the triplet state show a decrease in the Ge−Cl bond length by 0.016 Å with a large increase in the bond length of 18.4°. The singlet−triplet splitting of 61.4 kcal mol$^{-1}$ at the BHLYP level is in good agreement with Balasubramanian's CASSCF and MRSDCI results[42] of 59.5 kcal mol$^{-1}$ and 60.3 kcal mol$^{-1}$, respectively. For $GeCl_2$ the ZPVE corrected adiabatic electron affinities range from 1.50 to 1.70 eV in the order of BLYP < BHLYP < B3LYP, and the VEA and VDE values decrease by 0.39 and 0.95 eV, respectively, compared to $GeH_2$.

**H. $GeBr_2$ and $GeBr_2^-$.** The equilibrium geometries for the $^1A_1$ state of the neutral, the $^2B_1$ state of the anion $GeBr_2^-$, and the $^3B_1$ triplet state of $GeBr_2$ are presented in Figure 6. Between the ground state neutral and anion there is an increase in the bond length of 0.174 Å, and the bond angle is predicted to increase at the B3LYP and BLYP levels. This is not true for BHLYP, where a small decrease of 0.3° is predicted. The computed properties for the $^1A_1$ neutral ground state at the B3LYP level were in better agreement with Balasubramanian's highest level results than the CASSCF results.[42] The equilibrium geometry of the $^3B_1$ state reveals a decrease in the bond length by 0.024 Å, accompanying a large increase in the bond angle of 19.1°. The theoretical $EA_{ad(ZPVE)}$, VEA, and VDE results for $GeBr_2$ are shown in Tables 1−3. It may be noted that the predicted $EA_{ad(ZPVE)}$ ranges from 1.61 to 1.84 eV in the order BLYP < BHLYP ∼ B3LYP. The theoretical value for the singlet−triplet splitting of 54.8 kcal mol$^{-1}$ with the BHLYP functional is found to be in best agreement with Balasubramanian's value of 55.5 kcal mol$^{-1}$.[42] All energy differences between $EA_{ad(ZPVE)}$, VEA, and VDE are small, due to the slight differences in the geometries between the neutral and the anion. The B3LYP difference in $EA_{ad(ZPVE)}$ between $GeBr_2$ and $GeCl_2$ is 1.84 − 1.70 = 0.14 eV.

**I. $GeI_2$ and $GeI_2^-$.** The optimized geometries of the $^1A_1$ ground state neutral $GeI_2$, the $^2B_1$ state of the $GeI_2^-$ anion, and the $^3B_1$ triplet state $GeI_2$ are presented in Figure 7. The geometries of the neutral ground state $^1A_1$ $GeI_2$ with Ge−I bond length of 2.613 Å and bond angle of 103.5° obtained at the CASSCF level of theory[42] agree well with the present results obtained with the B3LYP functional. The theoretical $EA_{ad}$, $EA_{ad(ZPVE)}$, VEA, and VDE results are shown in Tables 1−3. The predicted $EA_{ad(ZPVE)}$ ranges from 1.77 to 2.07 eV, in the order BLYP < B3LYP ∼ BHLYP. It should be noted that though the 6-311G(d,p) basis sets was used for the iodine atom, this does not influence the relative trends for both the geometrical parameters and energy separations of $GeI_2$. The iodo substituents raise the VEA and VDE by 0.69 and 1.10 eV, respectively, compared to $GeH_2$. From Table 1, it is seen that there is a difference in the $EA_{ad(ZPVE)}$ of 0.20 eV between $GeBr_2$ and $GeI_2$. The energy splittings obtained with all three functionals, from Table 4, are found to be consistent with the energy separation of 45.5 kcal mol$^{-1}$ obtained at the CASSCF level of theory.[42] Table 5 lists the theoretical vibrational frequencies (cm$^{-1}$) for the $GeX_2$ species with $C_{2v}$ symmetry.

The results obtained for these germanium-containing species may be explained in terms of electron-withdrawal and $\pi$-donation abilities. Electronegative substituents withdraw electron density from the Ge, resulting in more positive "charge", making

**TABLE 4: Singlet−Triplet Gaps (eV) (kcal mol$^{-1}$ in parentheses)**

| | BH & HLYP | BLYP | B3LYP |
|---|---|---|---|
| **Ge**$H_2$ | 1.06 (24.4) | 1.23 (28.3) | 1.16 (26.7) |
| **Ge**$F_2$ | 3.57 (82.4) | 3.72 (85.9) | 3.69 (85.0) |
| **Ge**$Cl_2$ | 2.66 (61.4) | 2.83 (65.2) | 2.78 (64.1) |
| **Ge**$Br_2$ | 2.38 (54.8) | 2.52 (58.1) | 2.48 (57.2) |
| **Ge**$I_2$ | 2.08 (47.9) | 2.05 (47.2) | 2.07 (47.7) |
| **Ge**HF | 1.91 (44.0) | 2.05 (47.3) | 2.00 (46.2) |
| **Ge**HCl | 1.72 (39.7) | 1.87 (43.1) | 1.82 (42.0) |
| **Ge**HBr | 1.65 (38.1) | 1.79 (41.3) | 1.75 (40.3) |
| **Ge**HI | 1.53 (35.4) | 1.67 (38.5) | 1.63 (37.5) |
| **Ge**FCl | 3.07 (70.8) | 3.22 (74.4) | 3.18 (73.4) |
| **Ge**FBr | 2.88 (66.5) | 3.02 (69.7) | 2.99 (68.9) |
| **Ge**FI | 2.58 (59.5) | 2.71 (62.6) | 2.68 (61.8) |
| **Ge**ClBr | 2.51 (57.9) | 2.66 (61.4) | 2.62 (60.5) |
| **Ge**ClI | 2.26 (52.1) | 2.41 (55.6) | 2.37 (54.6) |
| **Ge**BrI | 2.15 (49.5) | 2.29 (52.8) | 2.25 (51.9) |
| H**Ge**$CH_3$ | 1.14 (26.4) | 1.29 (29.8) | 1.24 (28.5) |
| F**Ge**$CH_3$ | 2.01 (46.4) | 2.09 (48.3) | 2.08 (48.0) |
| Cl**Ge**$CH_3$ | 1.81 (41.8) | 1.91 (44.0) | 1.89 (43.5) |
| Br**Ge**$CH_3$ | 1.74 (40.1) | 1.83 (42.2) | 1.81 (41.7) |
| I**Ge**$CH_3$ | 1.60 (37.0) | 1.70 (39.3) | 1.68 (38.7) |
| H**Ge**$SiH_3$ | 0.73 (16.8) | 0.91 (21.1) | 0.84 (19.3) |
| H**Ge**$GeH_3$ | 0.79 (18.3) | 0.98 (22.6) | 0.91 (20.9) |
| F**Ge**$SiH_3$ | 1.26 (29.0) | 1.39 (32.2) | 1.35 (31.1) |
| F**Ge**$GeH_3$ | 1.31 (30.3) | 1.45 (33.5) | 1.41 (32.4) |
| Cl**Ge**$SiH_3$ | 1.15 (26.4) | 1.29 (29.7) | 1.24 (28.6) |
| Cl**Ge**$GeH_3$ | 1.19 (27.4) | 1.33 (30.7) | 1.29 (29.6) |
| Br**Ge**$SiH_3$ | 1.11 (25.6) | 1.25 (28.8) | 1.20 (27.7) |
| Br**Ge**$GeH_3$ | 1.15 (26.6) | 1.29 (29.8) | 1.25 (28.8) |
| I**Ge**$SiH_3$ | 1.03 (23.9) | 1.18 (27.1) | 1.13 (26.1) |
| I**Ge**$GeH_3$ | 1.08 (24.8) | 1.22 (28.2) | 1.17 (27.1) |
| $CH_3$**Ge**$SiH_3$ | 0.78 (18.0) | 0.95 (21.8) | 0.88 (20.3) |
| $CH_3$**Ge**$GeH_3$ | 0.85 (19.6) | 1.02 (23.5) | 0.96 (22.1) |
| **Ge**$(CH_3)_2$ | 1.26 (29.1) | 1.38 (31.9) | 1.34 (31.0) |
| **Ge**$(SiH_3)_2$ | 0.48 (11.0) | 0.68 (15.6) | 0.60 (13.8) |
| **Ge**$(GeH_3)_2$ | 0.57 (13.2) | 0.77 (17.8) | 0.69 (16.0) |

**TABLE 5: Theoretical Harmonic Vibrational Frequencies (cm$^{-1}$) for $GeX_2$ Species with $C_{2v}$ Symmetry**

| | | frequencies (cm$^{-1}$) | | |
|---|---|---|---|---|
| species | | neutral | anion | triplet |
| **Ge**$H_2$ | B3LYP | 937, 1885, 1894 | 877, 1701, 1708 | 815, 1992, 2084 |
| | BLYP | 905, 1807, 1818 | 845, 1621, 1633 | 789, 1888, 1993 |
| | BHLYP | 978, 1975, 1980 | 919, 1786, 1786 | 847, 2100, 2176 |
| **Ge**$F_2$ | B3LYP | 243, 630, 653 | 208, 489, 509 | 170, 607, 647 |
| | BLYP | 226, 595, 616 | 192, 461, 479 | 153, 554, 594 |
| | BHLYP | 263, 668, 694 | 227, 520, 543 | 189, 666, 704 |
| **Ge**$Cl_2$ | B3LYP | 147, 359, 380 | 105, 252, 283 | 103, 330, 376 |
| | BLYP | 136, 342, 360 | 97, 240, 269 | 92, 299, 343 |
| | BHLYP | 159, 375, 398 | 114, 261, 295 | 114, 361, 408 |
| **Ge**$Br_2$ | B3LYP | 95, 266, 274 | 67, 187, 207 | 69, 223, 281 |
| | BLYP | 89, 254, 260 | 62, 178, 196 | 62, 202, 257 |
| | BHLYP | 103, 278, 287 | 73, 193, 216 | 76, 244, 305 |
| **Ge**$I_2$ | B3LYP | 71, 219, 220 | 50, 156, 169 | 93, 126, 183 |
| | BLYP | 66, 208, 208 | 47, 149, 160 | 81, 124, 175 |
| | BHLYP | 77, 229, 231 | 54, 161, 176 | 104, 121, 189 |

the germanium a better $\pi$-acceptor, acquiring enhancement of the $\pi$-donation from the halo substituents. The electron affinities in the case of fluoro substituents decrease sharply, due to the shortness of the Ge−F bond. The fluorine lone pair crowds into the germanium $\pi$-orbital, indicating that $\pi$-donation dominates. For the chloro, bromo, and iodo substituents, the electron affinities increase in the order $GeH_2 < GeHX < GeX_2$, indicative of the major effect of electron withdrawal. The overall charge on the Ge atom is significantly positive in the case of $GeF_2$, as expected, due to the presence of the strongly electron withdrawing F atom; the 4s/4p population on Ge is particularly reduced. It is noted that in the $\sigma$ bond, the 4p contribution of the Ge atom is higher in the singlet states, whereas in the triplet states the 4s contribution of the Ge atom is less. This confirms that the $\sigma$ orbitals in the halo-substituted germylenes have antibonding character. The 4s germanium contribution to the sp$^n$ hybridization strongly decreases in going down the halogen group. Stabilization of the $\sigma$ nonbonding orbital by electron-withdrawing substituents increases the 4s character. This change in hybridization leads to a larger energy gap between the $\sigma^2 4p^0$ and $\sigma^1 4p^1$ states.

Our theoretical values obtained with the BHLYP functional for the $GeX_2$ series are consistent with Szabados and Hargittai's[60] CCSD(T)/ST findings, with minor differences in the geometrical parameters and singlet−triplet gaps. The trend observed in the different forms of electron affinities, for the series $GeH_2 < GeHX < GeX_2$, indicates that electron withdrawal is the major effect. However, in the case of the fluoro substituent there is an unexpected decrease in the $EA_{ad(ZPVE)}$, showing that there is a substantial amount of $\pi$-donation prevailing, as compared to the other halogens. This effect also reflects the contribution of the smaller size of the fluorine atom.

The significant increase in the positive charge on the divalent germanium center with fluoro substitution enhances the polarity of the Ge−F bond as well as the interelectron repulsion between the negatively charged halogen atoms. The $\sigma$ C−F bond is thus more polarized than the Ge−Cl, Ge−Br, and Ge−I bonds, and this implies that the polarizability effect is the dominant factor. This polarizability argument explains the poorer $\sigma$ withdrawing abilities of the Ge−Cl, Ge−Br, and Ge−I bonds and the less effective donor abilities of the nonbonding electron pairs on these halogen substituents and also accounts for the sizes of the chloro, bromo, and iodo substituents. This confirms that there are no large differences in the withdrawing abilities of the Ge−Cl/Br/I bonds.

**J. GeFCl, GeFBr, GeFI, GeClBr, GeClI, GeBrI.** The replacement of one fluorine atom of $GeF_2$ by a chloro substituent raises the $EA_{ad(ZPVE)}$ by 0.43 eV, the VEA by 0.36 eV, and the VDE by 0.53 eV. Conversely, replacement of one chlorine atom of $GeCl_2$ by a fluoro substituent decreases $EA_{ad(ZPVE)}$ by 0.36 eV, VEA by 0.33 eV, and VDE by 0.40 eV. Similarly, bromine monosubstitution increases $EA_{ad(ZPVE)}$ for difluorogermylene by 0.53 eV. Conversely, we predict a marked decrease in the $EA_{ad(ZPVE)}$ on substitution of a fluorine atom in dibromogermylene by 0.42 eV. Thus, contrary to accepted electronegativities, there is a general trend to raise EA values where a heavier halogen replaces a lighter halogen. This general trend for the increase in $EA_{ad(ZPVE)}$ is also seen going from $GeF_2$ to GeFI by 0.69 eV, VDE by 0.63 eV, and VEA by 0.79 eV (BHLYP). All geometrical parameters in this section may be found in the Supporting Information.[57]

The substitution of bromine into $GeCl_2$ raises the $EA_{ad(ZPVE)}$ by only 0.09 eV, the VEA by 0.09 eV, and the VDE by 0.08 eV, unlike chlorine atom substitution into $GeBr_2$ which decreases $EA_{ad(ZPVE)}$ by 0.07 eV, VEA by 0.09 eV, and the VDE by 0.06 eV. Again the general trend is confirmed.

**K. GeHF, GeHCl, GeHBr, GeHI, Their Neutral Ground States, Anions, and Triplet States.** The equilibrium geometries of the $^1A'$ state of neutral GeHX, the $^2A''$ state of the $GeHX^-$ anion, and the $^3A''$ triplet state of GeHX where X = F, Cl, Br, I are presented in Figures 8−11, so as to illustrate how a halogen substituent affects the electron affinity of germylene. For ground state $^1A'$ GeHF and its $^3A''$ triplet state, the decrease in the Ge−F bond length is only 0.012 Å, accompanying a large increase in the bond angle of 17.9°. Relative to $GeH_2$, monofluoro substitution reduces the $EA_{ad(ZPVE)}$ value by 0.08 eV and the VEA by

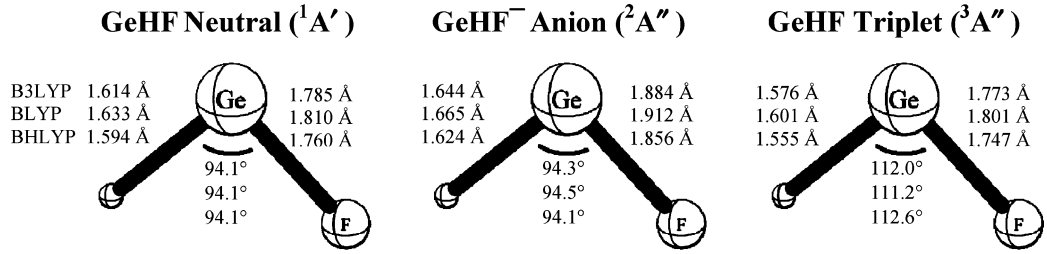


**Figure 8.** Equilibrium geometries of the $^1$A′ state of GeHF, $^2$A″ state of the GeHF$^-$ anion, and $^3$A″ state of the GeHF.

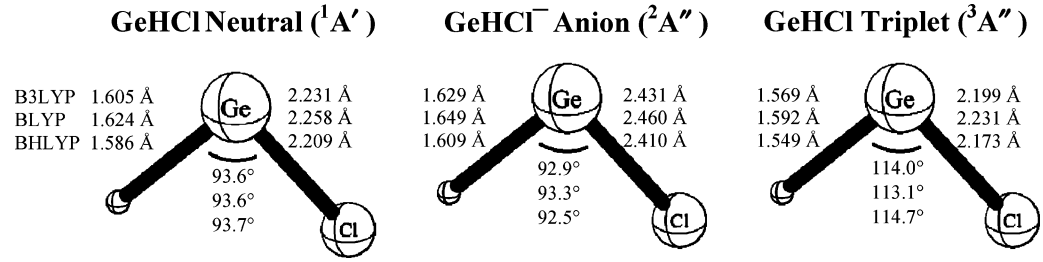


**Figure 9.** Equilibrium geometries of the $^1$A′ state of GeHCl, $^2$A″ state of the GeHCl$^-$ anion, and $^3$A″ state of the GeHCl.

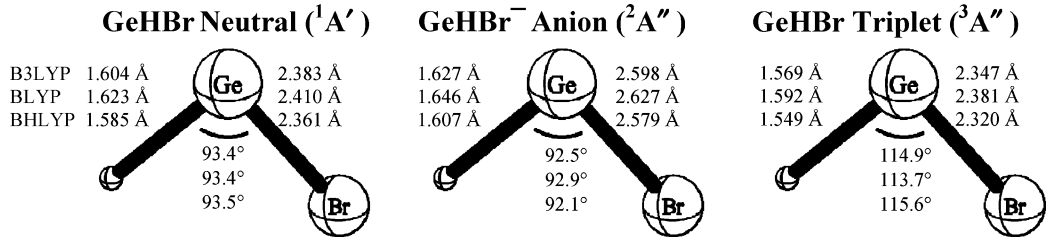


**Figure 10.** Equilibrium geometries of the $^1$A′ state of GeHBr, $^2$A″ state of the GeHBr$^-$ anion, and $^3$A″ state of the GeHBr.

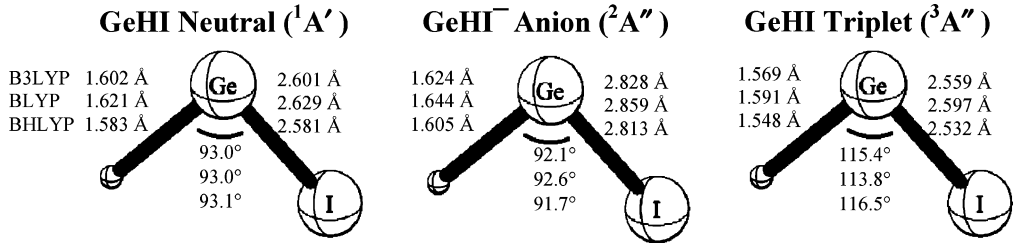


**Figure 11.** Equilibrium geometries of the $^1$A′ state of GeHI, $^2$A″ state of the GeHI$^-$ anion, and $^3$A″ state of the GeHI.

0.15 eV, with a small increase in the VDE by 0.02 eV. The singlet−triplet separations for all these species are listed in Table 4.

Balasubramanian et al.[42] has predicted the spectroscopic properties of GeHCl, GeHBr, and GeHI by the CASSCF and MRSDCI levels. Our theoretical results yield a Ge−Cl bond length of 2.231 Å and 1.605 Å for Ge−H and a bond angle of 93.6° for $^1$A′ GeHCl at the B3LYP level. These results were found to be comparable to the CASSCF results. Between the neutral and the anionic GeHCl, there are increases in the Ge−H and Ge−Cl bond lengths by 0.024 and 0.200 Å, respectively. The Ge−Cl and Ge−H bond lengths for the $^3$A″ triplet state differ from the neutral $^1$A′ ground state GeHCl by 0.032 and 0.036 Å, with a corresponding large increase in the bond angle of 20.4°. The singlet−triplet energy separation of 39.7 kcal mol$^{-1}$ was also found to be within 2 kcal mol$^{-1}$ with the previous theoretical result[42] of 37.7 kcal mol$^{-1}$.

In the case of GeHBr, it is predicted from Tables 1−3 that a bromo substituent increases the $EA_{ad(ZPVE)}$, VEA, and VDE by 0.37, 0.23, and 0.55 eV compared to $GeH_2$. Structural differences between the neutral and the anion correspond in an increase in the Ge−Br bond length by 0.215 Å and an increase in the Ge−H bond length of 0.023 Å, while the H−Ge−Br bond angle decreases by 0.9°. Comparing GeHI to $GeH_2$ reveals that substitution with a single iodine atom increases the $EA_{ad(ZPVE)}$, VEA, and VDE values of germylene by 0.47, 0.35, and 0.65 eV. The singlet−triplet energy splittings for GeHBr and GeHI correspond to 1.75 eV (40.3 kcal mol$^{-1}$) and 1.63 eV (37.5 kcal mol$^{-1}$), respectively. These values lie within 3 kcal mol$^{-1}$ of the previous Balasubramanian theoretical values obtained at the MRSDCI method.

Following standard Pauling electronegativities, the most electronegative substituents, F(3.98) > Cl(3.16) > Br(2.96) > I(2.66) > C(2.55) > H(2.20) > Ge(2.01) > Si(1.90),[61] tend to withdraw charge from the divalent germanium atom, leading to an increase in the central atom's positive charge. From the electronegativities, we expected the electron affinities for all species containing fluorine atom, in both series $GeX_2$ and GeXY, to be larger than the chloro, bromo, and iodo analogues, since the $\sigma$ acceptor ability of the halogen atom correlates linearly with its electronegativity. But this is not the case. Despite the fact that the electronegativities of the halogen atoms decrease in the order F > Cl > Br > I, the electron affinities increase in the opposite order. Hence, we conclude that electronegativity

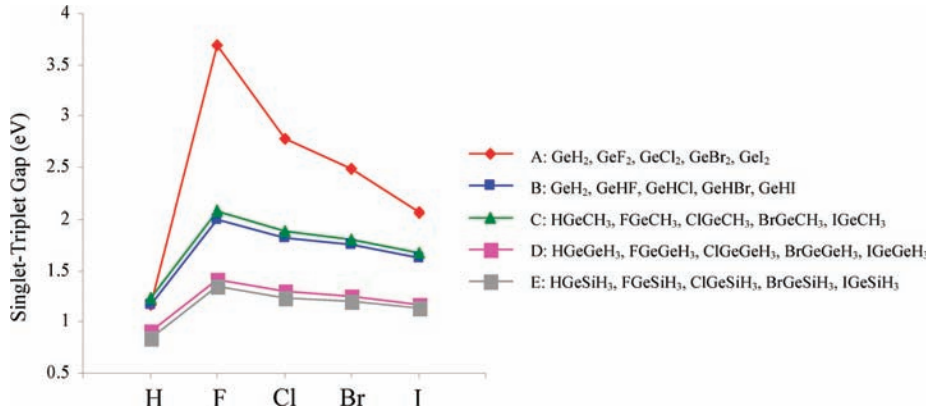


**Figure 12.** Graph of DZP++/B3LYP singlet−triplet splittings (eV) versus halogen substituents.

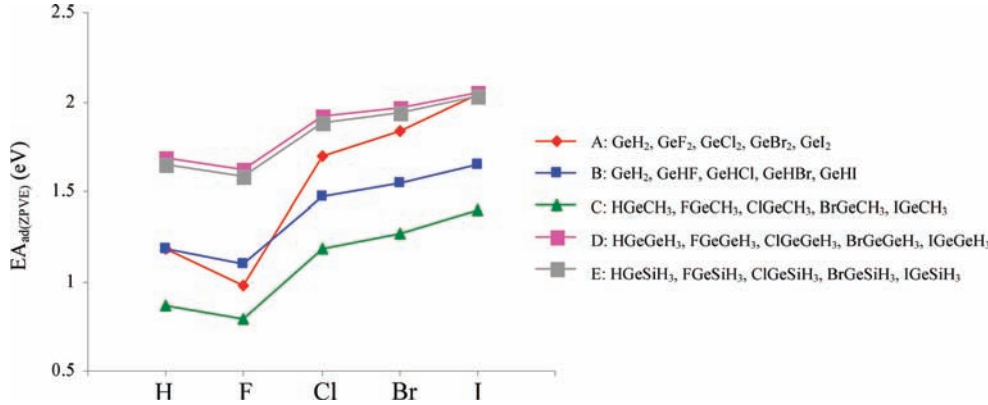


**Figure 13.** Graph of DZP++/B3LYP $EA_{ad(ZPVE)}$ (eV) versus halogen substituents.

is not the sole feature in determining the ability of germylenes to accept an extra electron. In essence the size of the central atom and of the halogen substituent, the electron density clouding the divalent center, and interelectron repulsion are the more decisive factors in influencing electron affinities.

**L. $XGeCH_3$ (Where X = H, F, Cl, Br, I), Their Anions and Triplet States.** To allow a comparative analysis of the halogen species, the electron affinities for $XGeCH_3$ are examined for X = H, F, Cl, Br, I. Relative to $HGeCH_3$, a single fluoro substituent X decreases the $EA_{ad(ZPVE)}$ by 0.05 eV and the VEA by 0.11 eV, with a small increase in the VDE of 0.03 eV. Proceeding down the halogen group, Tables 1−3 clearly demonstrate the increasing electron affinities. In order to compare the effect of the fluoro and methyl substituents, we consider the $EA_{ad(ZPVE)}$ values of GeHF = 0.98 eV and $GeHCH_3$ = 0.69 eV (BHLYP). From these predicted values, it is noted that there is a more pronounced effect on the $EA_{ad(ZPVE)}$ with replacement of the fluorine atom by the electron-donating $CH_3$ group, thus causing the positive charge density of the central atom to decrease considerably. Hence the ability of the $XGeCH_3$ (X = H, F, Cl, Br, I) species to accommodate an extra electron is even weaker. Figures 12 and 13 summarize the effects of halogen substituents on the singlet−triplet splittings and the $EA_{ad(ZPVE)}$ at the DZP++/B3LYP level.

## IV. Discussion

This section compares the present predictions for the germanium-containing species with their carbon and silicon analogues.

**(i) Structures, Singlet and Triplet Gaps.** The structural parameters for the carbon and silicon analogues, available in the experimental literature, are collected in Table 6, along with the few available electron affinities and singlet−triplet gaps. The similarities observed for the series $CX_2 \rightarrow SiX_2 \rightarrow GeX_2$ are reflected in the fact that all have closed-shell singlet electronic ground states. This means $A_1$ symmetry for all $C_{2v}$ molecules and A′ symmetry for the $C_s$ point groups. The lowest-lying triplet states have $B_1$ spatial symmetry for all $C_{2v}$ symmetries and A″ symmetry for all $C_s$ symmetries. Previously Apeloig et al.[62] discussed the fact methylene has a ground state triplet, in contrast to silylene and germylene being ground state singlets. For the F/Cl/Br/I−halocarbenes, the singlet states are characterized by smaller bond angles in their ground states,[60,63] while significantly larger bond angles are predicted for their lowest-lying triplet states. The deviation from the ideal singlet bond angle, 120°, is mainly due to repulsion by the lone pair of electrons of the divalent carbene, whose effect is much greater than the repulsion of the bonding electron pair. The resulting repulsion between the carbene lone pair and the halogens lengthens the bond distances slightly. Previous theoretical studies have predicted that in general carbene/silylene/germylene, upon excitation of an electron from the singlet ground state to their respective low-lying triplet state, the C/Si/Ge−halogen bond lengths show relatively smaller changes while the divalent angles increase largely from ∼97−112° to ∼115−135°.[63]

The analysis of geometrical parameters revealed comparatively regular trends with an increase in the electronegativity of the halogen substituent. The determination of the multiplicity of the ground state and the extent of singlet−triplet separation depend upon factors such as the sp hybridization of the $\sigma$ orbitals and the electronegativity of the substituents. Within each series $CX_2$/CXY and $SiX_2$/SiXY there is an excellent linear relationship between the singlet−triplet gap and the substituent electronegativity with the same halogen atom.

**TABLE 6: Experimental Structural Parameters, Singlet−Triplet Gaps, Electron Affinities (eV) for the Carbon and Silicon Analogues**

| M | C | Si |
|---|---|---|
| $MH_2$ | $r$(C−H) = 1.078 Å, ∠(H−C−H) = 136.0° [72]<br>$r$(C−H) = 1.077 Å, ∠(H−C−H) = 134.0° [73]<br>$r$(C−H) = 1.107 Å, ∠(H−C−H) = 102.4° [74]<br>$\Delta E_{S\text{-}T}$ = 9.09 ± 0.20 kcal mol$^{-1}$ [73]<br>EA = 0.6520 ± 0.0060 kcal mol$^{-1}$ [68]<br>EA = 0.210 ± 0.015 kcal mol$^{-1}$ [69]<br>EA = 0.208 ± 0.031 kcal mol$^{-1}$ [70]<br>EA > 0.90 ± 0.40 kcal mol$^{-1}$ [71] | $r$(Si−H) = 1.514 Å, ∠(H−Si−H) = 92.1° [90]<br>$r$(Si−H) = 2.861 Å, ∠(H−Si−H) = 92.0° [91]<br>EA = 1.123 ± 0.022 kcal mol$^{-1}$ [92] |
| $MF_2$ | $r$(C−F) = 1.304 Å, ∠(F−C−F) = 104.8° [75]<br>$r$(C−F) = 1.300 Å, ∠(F−C−F) = 104.9° [99]<br>$\Delta E_{S\text{-}T}$ = 237.14 ± 0.02 kJ mol$^{-1}$ [76]<br>EA = 0.180 ± 0.020 kcal mol$^{-1}$ [87]<br>EA = 0.1790 ± 0.0050 kcal mol$^{-1}$ [77]<br>EA = 0.07 ± 0.15 kcal mol$^{-1}$ [79]<br>EA < 1.30 ± 0.80 kcal mol$^{-1}$ [80]<br>EA > 0.2005 kcal mol$^{-1}$ [81]<br>EA = 2.6495 kcal mol$^{-1}$ [82] | $r$(Si−F) = 1.590 Å, ∠(F−Si−F) = 100.8° [93]<br>$r$(Si−F) = 1.586 Å, ∠(F−Si−F) = 113.1° [94]<br>EA = 0.10 ± 0.10 kcal mol$^{-1}$ [95] |
| $MCl_2$ | $r$(C−Cl) = 1.716 Å, ∠(Cl−C−Cl) = 109.2° [83]<br>$r$(C−Cl) = 1.714 Å, ∠(Cl−C−Cl) = 109.3° [84] | $r$(Si−Cl) = 2.088 Å, ∠(Cl−Si−Cl) = 102.8° [96]<br>$r$(Si−Cl) = 2.041 Å, ∠(Cl−Si−Cl) = 114.5° [97]<br>EA = 0.77 ± 0.13 kcal mol$^{-1}$ [45] |
| $MBr_2$ | $r$(C−Br) = 1.740 Å, ∠(Br−C−Br) = 112.0° [85]<br>EA = 1.928 ± 0.082 kcal mol$^{-1}$ [86]<br>EA = 1.880 ± 0.070 kcal mol$^{-1}$ [87] | $r$(Si−Br) = 2.249 Å, ∠(Br−Si−Br) = 102.7° [96]<br>EA > 1.7 kcal mol$^{-1}$ [45] |
| MHF | $r$(C−H) = 1.138 Å, $r$(C−F) = 1.305 Å [88]<br>$\Delta E_{S\text{-}T}$ = 62.3 ± 1.7 kJ mol$^{-1}$ [76]<br>$\Delta E_{S\text{-}T}$ = 14.9 ± 0.4 kcal mol$^{-1}$ [89]<br>$\Delta E_{S\text{-}T}$ = 11.4 ± 0.3 kcal mol$^{-1}$ [77]<br>EA = 0.5570 ± 0.0050 kcal mol$^{-1}$ [77]<br>EA = 0.5420 ± 0.0050 kcal mol$^{-1}$ [89] | |
| MHCl | $\Delta E_{S\text{-}T}$ = 17.6 ± 10.5 kJ mol$^{-1}$ [76,89]<br>EA = 1.2100 ± 0.0050 kcal mol$^{-1}$ [89]<br>EA = 1.2130 ± 0.0050 kcal mol$^{-1}$ [77] | |
| MHBr | $r$(C−H) = 1.116 Å, $r$(C−Br) = 1.854 Å,<br>∠(H−C−Br) = 104.1° [98]<br>$\Delta E_{S\text{-}T}$ = 10.9 ± 9.2 kJ mol$^{-1}$ [76,89]<br>EA = 1.5560 ± 0.0080 kcal mol$^{-1}$ [77]<br>EA = 1.6800 ± 0.0050 kcal mol$^{-1}$ [89]<br>EA = 1.683 ± 0.012 kcal mol$^{-1}$ [77] | |

Consistent with the earlier work by Irikura et al.[64] on the singlet−triplet gaps of substituted carbenes CXY (X, Y = H, F, Cl, Br, I, $SiH_3$), the singlet−triplet gaps correlate with the charge and electronegativity of the substituents. The computational study of the molecular structures for the carbene and silylene analogues by Szabados and Hargittai[60] predicts a similar variation in both the geometrical parameters and singlet−triplet gaps. The ab initio calculations reported by different workers[63,65−67] for the ground and excited electronic states for carbenes predict comparable trends in geometrical parameters and singlet−triplet splittings. The theoretical trends in bond lengths and bond angle for the germanium-containing species are consistent with those observed for the carbon and silicon analogues.

The dihalo-substituted silylenes, SiHX, where X = F, Cl, Br, and I, have substantially larger singlet−triplet gaps, for any given angle, reflecting greater $\pi$-donation. The dependence of singlet−triplet gaps upon bond angle, gives further support for $\pi$-donation. The opening of the bond angle modifies the hybridization of the central divalent atom. The trend predicted in the bond lengths for the series, C → Si → Ge, from H → F → Cl → Br → I, is of course dependent on the atomic sizes of the halogen substituents.

For the singlet $^1A'$ ground state of SiXY, the HOMO is of a′ symmetry, corresponding to the lone pair of electrons lying in the molecular plane, occupying a large space, and therefore resulting in bond angles less than 120°. In the triplet state a single electron is moved to an A″ orbital, which is the out-of-plane p orbital of the divalent center. The a′ orbital is a $\sigma$-type antibonding orbital contributing to the in-plane p orbitals of the substituents in opposite phase. Hence, only one electron occupies the central atom, leading to a decrease in repulsion and increase in bond angle as compared to their respective singlet states. With the decreasing electronegativity of the halo substituents, the contribution of the s orbital to the $a_1$ molecular orbital decreases, hence raising its energy. For the triplet states, with decreasing electronegativity and increasing size of the halo substituent, the energy of the out-of-plane p orbital increases and the overlapping of these orbitals with the silicon p orbital decreases together with a decrease in the energy of the antibonding nature of the $b_1$ orbital. In going from F → Cl → Br → I, the $b_1$ and a″ orbitals get closer to each other, and their energy separation decreases.

**(ii) Electron Affinities.** Comparing the geometrical parameters and electron affinities of the carbene series to the corresponding silicon hydride analogues shows important differences. From the literature, early experimental values for the electron affinity of methylene vary from 0.20 to >0.90 eV,[68−71] and recently Furtenbacher et al.[101] stated that the methylene saga continues. From Leopold et al.,[68] $CH_2$ has a reliable experimental EA = 0.652 eV, to be compared to Kasdan, Herbst, and Lineberger's laser photoelectron spectroscopy results for $SiH_2$

$= 1.124 \pm 0.020$ eV.[92] Silicon has a much larger p orbital than carbon and carbon has a larger s orbital than silicon.[60] The disparity in EAs for $CH_2$ and $SiH_2$ is due an extra electron which adds to a singly occupied $a_1$ orbital in $CH_2$ but adds to an unoccupied, nonbonding $b_1$ orbital in $SiH_2$.[60] The experimental electron affinities for $CF_2$ of Schwartz et al. ($0.18 \pm 0.02$ eV)[87] and Murray et al. ($0.179 \pm 0.005$ eV)[77] are to be consistent, where the large decrease in the EA also indicates the dramatic effect of the fluoro substituent. Even $SiF_2$, in fact, displays a large decrease (compared to $SiH_2$) in the experimental EA, to values as low as $0.10 \pm 0.10$ eV. Consistent with Larkin's findings[47] for the silicon analogues, the predicted adiabatic electron affinity (AEA) for $SiF_2$ is 0.41 eV and that for SiHF is 0.76 eV (BHLYP). In general, geometrical parameters for germanium-containing species and the different forms of electron affinities follow the same trends as those of the silicon analogues.[47] It has been observed that the DZP++ $EA_{zero}$[47,59,78] for $SiH_2$ predicted with the BHLYP functional almost identically reproduces the available experimental value, as seen in Table 6. The series $XSiCH_3$ ($X$ = H, F, Cl, Br) also shows the same effect for the electron affinities.

Reliable experimental values for the electron affinities are lacking for most of the germanium-containing species considered. Compared to the neutral series, experimental data on the singly charged anions and singlet−triplet splittings and the geometrical properties are scarce for $XGeMH_3$ (X = H, F, Cl, Br, I; M = C, Si, Ge). In keeping with Larkin's findings[47] for the silicon analogues, it is observed that the methyl substituents significantly decrease the electron affinities.

A fairly similar trend in the electron affinities may also be observed while descending group IV for the series $HGeMH_3$ (M = C, Si, Ge). This reflects the fact that the electronegativity of silicon (1.90) is lower than that of germanium (2.01). From C → Si → Ge, the internuclear distance increases; hence the electron donor ability of the $MH_3$ moiety varies considerably in the series $HGeCH_3 \gg HGeSiH_3 > HGeGeH_3$, where the predicted $EA_{ad(ZPVE)}$ are 0.71, 1.51, and 1.55 eV, respectively. The trend observed for the $SiH_3$ and $GeH_3$ moieties is notably comparable. Consequently, the effect of the inductively withdrawing group, $CH_3$, is significantly enhanced compared to the $SiH_3$ and $GeH_3$ groups. Consistent with the theoretical values for the silicon analogues, the methyl substituents present a significant dip in the AEA compared to that effected by fluorine atom. For comparison purposes the AEA for silicon analogues obtained with the BHLYP functional are included in Table 1. This shows that the Ge−Si and Ge−Ge bonds are somewhat better $\sigma$ acceptors than the Ge−C bond. Similarly, a halogen atom attached to the divalent center M = C, Si, and Ge for the series $HGeMH_3$ has the same effect as that predicted in the electron affinities for $GeX_2$ (X = F, Cl, Br, I) when going from F → Cl → Br → I.

## V. Conclusion

In this research, $GeX_2$ and GeXY species have been investigated, including many yet unobserved structures. Consistent with the silicon analogues, it is concluded that dimethylgermylene also binds an electron, though weakly, with the electron affinity ranging from 0.44 eV (BHLYP) to 0.60 eV (B3LYP). The increasing ability of halogens to bind an electron, going down the periodic table, is established, with the iodo substituent having the most dramatic effect in increasing the electron affinities. The $GeH_3$ and $SiH_3$ groups behave similarly and increase the germylene electron affinities versus $CH_3$ substitution. The largest singlet−triplet gap, ranging from 3.57 to 3.72 eV, is predicted for $GeF_2$, with $Ge(GeH_3)_2$ having the smallest splitting, ranging from 0.57 to 0.77 eV in the order of BHLYP < B3LYP < BLYP. The BHLYP functional provides the best agreement of the predicted structures with experimental geometrical parameters. The same functional is found to be the most reliable in predicting electron affinities when the results from this work are compared to experimental literature values. These observations have also been found for the silylene derivatives.[47] These may be correlated with the fact that the BHLYP functional incorporates the largest fraction of the Hartree−Fock method.[50] As found earlier for $Si(CH_3)_2$, no neutral structure of $C_{2v}$ symmetry was found for $Ge(CH_3)_2$ to be a minimum on the potential energy surface. It is noted that the singlet−triplet splittings for the germylenes are consistently larger than those for the methylene and silylene analogues.

**Acknowledgment.** The authors thank the reviewers for their helpful comments on the manuscript. The research has been supported by the Mauritius Tertiary Education Commission (TEC) and the U.S. National Science Foundation, Grant CHE-0749868. A.B. acknowledges the use of facilities at the University of Mauritius. We thank Dr. Andrew Simmonett and Jeremiah Wilke for helpful discussions.

**Supporting Information Available:** Geometrical parameters for 35 compounds. This material is available free of charge via the Internet at http://pubs.acs.org.

## References and Notes

(1) Tokitoh, N.; Okazaki, R. *Coord. Chem. Rev.* **2000**, *210*, 251.
(2) Kühl, O. *Coord. Chem. Rev.* **2004**, *248*, 411.
(3) Holl, M. B.; Peck, D. R. *Encyclopedia of Inorganic Chemistry*; King, R. B., Ed.; Wiley: Chichester, 2005; pp 1650−1673.
(4) Parr, J. *Annu. Rep. Prog. Chem., Sect. A* **2007**, *103*, 90.
(5) Kobayashi, S.; Iwata, S.; Hiraishi, M. *J. Am. Chem. Soc.* **1994**, *116*, 6047.
(6) Arduengo, A. J.; Bock, H.; Chen, H.; Denk, M.; Dixon, D. A.; Green, J. H.; Herrmann, W. A.; Jones, N. L.; Wagner, M.; West, R. *J. Am. Chem. Soc.* **1994**, *116*, 6641.
(7) Karolczak, J.; Harper, W. W.; Grev, R. S.; Clouthier, D. J. *J. Chem. Phys.* **1995**, *103*, 2839.
(8) Kobayashi, S.; Iwata, S.; Abe, M.; Shoda, S. *J. Am. Chem. Soc.* **1995**, *117*, 2187.
(9) Boehme, C.; Frenking, G. *J. Am. Chem. Soc.* **1996**, *118*, 2039.
(10) Gehrhus, B.; Hitchcock, P. B.; Lappert, M. F. *Angew. Chem., Int. Ed.* **1997**, *36*, 2514.
(11) Stogner, S. M.; Grev, R. S. *J. Chem. Phys.* **1998**, *108*, 5458.
(12) Su, M.-D.; Chu, S.-Y. *J. Am. Chem. Soc.* **1999**, *121*, 4229.
(13) Miller, K. A.; Bartolin, J. M.; O'Neill, R. M.; Sweeder, R. D.; Owens, T. M.; Kampf, J. W.; Holl, M. M. B.; Wells, N. J. *J. Am. Chem. Soc.* **2003**, *125*, 8986.
(14) Iwamoto, T.; Masuda, H.; Ishida, C.; Kira, M. *J. Am. Chem. Soc.* **2003**, *125*, 9300.
(15) Leites, L. A.; Bukalov, S. S.; Zabula, A. V.; Garbuzova, I. A.; Moser, D. A.; West, R. *J. Am. Chem. Soc.* **2004**, *126*, 4114.
(16) Pineda, L. W.; Jancik, V.; Roesky, H. W.; Neculai, D.; Necular, A. M. *Angew. Chem., Int. Ed.* **2004**, *43*, 1419.
(17) Leigh, W. J.; Harrington, C. R.; Vargas-Baca, I. *J. Am. Chem. Soc.* **2004**, *126*, 16105.
(18) Pineda, L. W.; Jancik, V.; Roesky, H. W.; Herbst-Irmer, R. *Angew. Chem., Int. Ed.* **2004**, *43*, 5534.
(19) Leigh, W. J.; Harrington, C. R. *J. Am. Chem. Soc.* **2005**, *127*, 5084.
(20) Olah, J.; De Proft, F.; Veszpremi, T.; Geerlings, P. *J. Phys. Chem. A* **2005**, *109*, 1608.
(21) Tumanskii, B.; Pine, P.; Apeloig, Y.; Hill, N. J.; West, R. *J. Am. Chem. Soc.* **2005**, *127*, 8248.
(22) Driess, M.; Yao, S.; Brym, M.; van Wullen, C. *Angew. Chem., Int. Ed.* **2006**, *45*, 4349.
(23) Gans-Eichler, T.; Gudat, D.; Nättinen, K.; Neiger, M. *Chem.—Eur. J.* **2006**, *12*, 1162.
(24) Li, W.; Hill, N. J.; Tomasik, A. C.; Bikzhanova, G.; West, R. *Organometallics* **2006**, *25*, 3802.
(25) Ullah, F.; Bajor, G.; Veszpremi, T.; Jones, P. G.; Heinicke, J. W. *Angew. Chem., Int. Ed.* **2007**, *46*, 2697.

(26) Xu, Y.-J.; Zhang, Y.-F.; Li, J.-Q. *J. Phys. Chem. C* **2007**, *111*, 3729.
(27) Rupar, P. A.; Staroverov, V. N.; Ragogna, P. J.; Baines, K. M. *J. Am. Chem. Soc.* **2007**, *129*, 15138.
(28) Al-Ktaifani, M. M.; Hitchcock, P. B.; Lappert, M. F.; Nixon, J. F.; Uiterweerd, P. *Dalton Trans.* **2008**, 2825.
(29) Hahn, F. E.; Zabula, A. V.; Pape, T.; Hepp, A.; Tonner, R.; Haunschild, R.; Frenking, G. *Chem.—Eur. J.* **2008**, *14*, 10716.
(30) Yao, S.; van Wullen, C.; Driess, M. *Chem. Commun.* **2008**, 5393.
(31) Nagendran, S.; Roesky, H. W. *Organometallics* **2008**, *27*, 457.
(32) Yao, S.; van Willen, C.; Driess, M. *Chem. Commun.* **2008**, 5393.
(33) Rupar, P. A.; Staroverov, V. N.; Baines, K. M. *Science* **2008**, *322*, 1360.
(34) Lieberman, M. A.; Lichtenberg, A. J. *Principles of Plasma Discharges and Materials Processing*; Wiley: New York, 2005.
(35) Claeys C. Simoen E. *Germanium-Based Technologies, from Materials to Devices*; Elsevier: Amsterdam, 2007.
(36) Balasubramanian, K. *J. Chem. Phys.* **1988**, *89*, 5731.
(37) Das, K. K.; Balasubramanian, K. *J. Chem. Phys.* **1990**, *93*, 5883.
(38) Li, Q.-S.; Lu, R.-H.; Xie, Y.; Schaefer, H. F. *J. Comput. Chem.* **2002**, *23*, 1642.
(39) Miller, T. M.; Miller, A. E. S.; Lineberger, W. C. *Phys. Rev. A* **1986**, *35*, 3558.
(40) Ito, H.; Hirota, E. *Chem. Phys. Lett.* **1991**, *177*, 235.
(41) Ito, H.; Hirota, E.; Kuchitsu, K. *Chem. Phys. Lett.* **1990**, *175*, 384.
(42) Benavides-Garcia, M.; Balasubramanian, K. *J. Chem. Phys.* **1992**, *97*, 10.
(43) Dai, D.; Al-Zahrani, M. M.; Balasubramanian, K. *J. Chem. Phys.* **1994**, *98*, 9233.
(44) Takeo, H.; Curl, R. F.; Wilson, P. W. *J. Mol. Spectrosc.* **1971**, *38*, 464.
(45) Pabst, R. E.; Margrave, J. L.; Franklin, J. L. *Int. J. Mass Spectrom. Ion Phys.* **1977**, *25*, 361.
(46) Sherrill, C. D.; Van Huis, T. J.; Yamaguchi, Y.; Schaefer, H. F. *J. Mol. Struct.* **1997**, *400*, 139.
(47) Larkin, J. D.; Schaefer, H. F. *J. Chem. Phys.* **2004**, *121*, 9361.
(48) Frisch, M. J.; Trucks, G. W.; Schlegel, H. B.; Scuseria, G. E.; Robb, M. A.; Cheeseman, J. R.; Montgomery, J. A., Jr.; Vreven, T.; Kudin, K. N.; Burant, J. C.; Millam, J. M.; Iyengar, S. S.; Tomasi, J.; Barone, V.; Mennucci, B.; Cossi, M.; Scalmani, G.; Rega, N.; Petersson, G. A.; Nakatsuji, H.; Hada, M.; Ehara, M.; Toyota, K.; Fukuda, R.; Hasegawa, J.; Ishida, M.; Nakajima, T.; Honda, Y.; Kitao, O.; Nakai, H.; Klene, M.; Li, X.; Knox, J. E.; Hratchian, H. P.; Cross, J. B.; Adamo, C.; Jaramillo, J.; Gomperts, R.; Stratmann, R. E.; Yazyev, O.; Austin, A. J.; Cammi, R.; Pomelli, C.; Ochterski, J. W.; Ayala, P. Y.; Morokuma, K.; Voth, G. A.; Salvador, P.; Dannenberg, J. J.; Zakrzewski, V. G.; Dapprich, S.; Daniels, A. D.; Strain, M. C.; Farkas, O.; Malick, D. K.; Rabuck, A. D.; Raghavachari, K.; Foresman, J. B.; Ortiz, J. V.; Cui, Q.; Baboul, A. G.; Clifford, S.; Cioslowski, J.; Stefanov, B. B.; Liu, G.; Liashenko, A.; Piskorz, P.; Komaromi, I.; Martin, R. L.; Fox, D. J.; Keith, T.; Al-Laham, M. A.; Peng, C. Y.; Nanayakkara, A.; Challacombe, M.; Gill, P. M. W.; Johnson, B.; Chen, W.; Wong, M. W.; Gonzalez, C.; Pople, J. A. *Gaussian 03, Revision C.02*; Gaussian Inc.: Wallingford, CT, 2004.
(49) Becke, A. D. *J. Chem. Phys.* **1988**, *38*, 3098.
(50) Becke, A. D. *J. Chem. Phys.* **1993**, *98*, 1372.
(51) Lee, C.; Yang, W.; Parr, R. G. *Phys. Rev. B* **1988**, *37*, 785.
(52) Huzinaga, S. *J. Chem. Phys.* **1965**, *42*, 1293.
(53) Dunning T. H.; Hay P. J. In *Modern Theoretical Chemistry*; Schaefer, H. F., Ed.; Plenum: New York, 1977; Vol. 3, p 1.
(54) Huzinaga S. *Approximate Atomic Wavefunctions II*; University of Alberta: Edmonton, Alberta, 1971.
(55) Lee, T. J.; Schaefer, H. F. *J. Chem. Phys.* **1985**, *83*, 1784.
(56) Schafer, A.; Horn, H.; Ahlrichs, R. *J. Chem. Phys.* **1992**, *97*, 2571.
(57) Supplementary Material.
(58) Harland, P. W.; Cradock, S.; Thynne, J. C. *J. Int. J. Mass Spectrom. Ion Phys.* **1972**, *10*, 169.
(59) Li, Q.; Li, G.; Xu, W.; Xie, Y.; Schaefer, H. F. *J. Chem. Phys.* **1999**, *111*, 7945.
(60) Szabados, A.; Hargittai, M. *J. Phys. Chem. A* **2003**, *107*, 4314.
(61) Allfred, A. L. *J. Inorg. Nucl. Chem.* **1961**, *17*, 215.
(62) Apeloig, Y.; Pauncz, R.; Karni, M.; West, R.; Steiner, W.; Chapman, D. *Organometallics* **2003**, *22*, 3250. For earlier work, see: O'Neil, S. V.; Schaefer, H. F.; Bender, C. F. *J. Chem. Phys.* **1971**, *55*, 162.
(63) Schwartz, M.; Marshall, P. *J. Phys. Chem. A* **1999**, *103*, 7900.
(64) Irikura, K. K.; Goddard, W. A.; Beauchamp, J. L. *J. Am. Chem. Soc.* **1992**, *114*, 48.
(65) Drake, S. A.; Standard, J. M.; Quandt, R. W. *J. Phys. Chem. A* **2002**, *106*, 1357.
(66) Lee, E. P. F.; Dyke, J. M.; Wright, T. G. *Chem. Phys. Lett.* **2000**, *326*, 143.
(67) Standard, J. M.; Quandt, R. W. *J. Phys. Chem. A* **2003**, *107*, 6877.
(68) Leopold, D. G.; Murray, K. K.; Miller, A. E. S.; Lineberger, W. C. *J. Chem. Phys.* **1985**, *83*, 4849.
(69) Engelking, P. E.; Corderman, R. R.; Wenddoski, J. J.; Ellison, G. B.; O'Neil, S. V.; Lineberger, W. C. *J. Chem. Phys.* **1981**, *74*, 5460.
(70) Zittel, P. F.; Ellison, G. B.; O'Neil, S. V.; Herbst, E.; Lineberger, W. C.; Reinhardt, W. P. *J. Am. Chem. Soc.* **1976**, *98*, 3731.
(71) Thynne, J. C. J.; MacNiel, K. A. G. *J. Phys. Chem.* **1971**, *75*, 2584.
(72) Herzberg, G.; Johns, J. W. C. *J. Chem. Phys.* **1971**, *54*, 2276.
(73) Bunker, P. R.; Jensen, P.; Kraemer, W. P.; Beardsworth, R. *J. Chem. Phys.* **1986**, *85*, 3724.
(74) Petek, H.; Nesbitt, D. J.; Darwin, D. C.; Ogilby, P. R.; Moore, C. B.; Ramsay, D. A. *J. Chem. Phys.* **1989**, *91*, 6566.
(75) Kirchhoff, W. H.; Lide, D. R.; Powell, F. X. *J. Mol. Spectrosc.* **1973**, *47*, 491.
(76) Jacox, M. E. *J. Phys. Chem. Ref. Data* **1998**, *27*, 115.
(77) Murray, K. K.; Leopold, D. G.; Miller, T. M.; Lineberger, W. C. *J. Chem. Phys.* **1988**, *89*, 5442.
(78) Pak, C.; Rienstra-Kiracofe, J.; Schaefer, H. F. *J. Phys. Chem. A* **2000**, *104*, 11232.
(79) Born, M.; Ingemann, S.; Nibbering, N. M. M. *J. Am. Chem. Soc.* **1994**, *116*, 7210.
(80) Harland, P. W.; Thynne, J. C. J. *Int. J. Mass Spectrom. Ion Phys.* **1972**, *10*, 11.
(81) Thynne, J. C. J.; MacNeil, K. A. G. *Int. J. Mass Spectrom. Ion Phys.* **1970**, *5*, 329.
(82) Page, F. M.; Goode, G. C. *Negative Ions and the Magnetron*; Wiley: New York, 1969.
(83) Fujitake, M.; Hirota, E. *J. Chem. Phys.* **1989**, *91*, 3426.
(84) Clouthier, D. J.; Karolczak, J. *J. Phys. Chem.* **1989**, *93*, 7542.
(85) Ivey, R. C.; Schulze, P. D.; Leggett, T. L.; Kohl, D. A. *J. Chem. Phys.* **1974**, *60*, 3174.
(86) Born, M.; Ingemann, S.; Nibbering, N. M. M. *Int. J. Mass Spectrom.* **2000**, *194*, 103.
(87) Schwartz, R. L.; Davico, G. E.; Ramond, T. M.; Lineberger, W. C. *J. Phys. Chem. A* **1999**, *103*, 8213.
(88) Suzuki, T.; Saito, S.; Hirota, J. *J. Mol. Spectrosc.* **1981**, *90*, 447.
(89) Gilles, M. K.; Ervin, K. M.; Ho, J.; Lineberger, W. C. *J. Phys. Chem.* **1992**, *96*, 1130.
(90) Yamada, C.; Kanamori, H.; Hirota, E.; Nishiwaki, N.; Itabashi, N.; Kato, K.; Goto, T. *J. Chem. Phys.* **1989**, *91*, 4582.
(91) Dubois, I. *Can. J. Phys.* **1968**, *46*, 2485.
(92) Kasdan, A.; Herbst, E.; Lineberger, W. C. *J. Chem. Phys.* **1975**, *62*, 541.
(93) Shoji, H.; Tanaka, T.; Hirota, E. *J. Mol. Spectrosc.* **1973**, *47*, 268.
(94) Karolczak, J.; Judge, R. H.; Clouthier, D. J. *J. Am. Chem. Soc.* **1995**, *117*, 952.
(95) Kawamata, H.; Negishi, Y.; Kishi, R.; Iwata, S.; Nakajima, A.; Kaya, K. *J. Chem. Phys.* **1996**, *105*, 5369.
(96) Hargittai, I.; Schultz, G.; Tremmel, J.; Kagramanov, N. D.; Maltsev, A. K.; Nefedov, O. M. *J. Am. Chem. Soc.* **1983**, *105*, 2895.
(97) Chau, F.-T.; Wang, D.-C.; Lee, E. P. F.; Dyke, J. M.; Mok, D. K. W. *J. Phys. Chem. A* **1999**, *103*, 4925.
(98) Marr, A. J.; North, S. W.; Sears, T. J.; Ruslen, L.; Field, R. W. *J. Mol. Spectrosc.* **1998**, *188*, 68.
(99) Mathews, C. W. *Can. J. Phys.* **1967**, *45*, 2355.
(100) Jensen, P.; Bunker, P. R. *J. Chem. Phys.* **1988**, *89*, 1327.
(101) Furtenbachera, T.; Czakó, G.; Sutcliffe, B. T.; Császár, A. G.; Szalay, V. *J. Mol. Struct.* **2006**, *283*, 780.
(102) Kutzelnigg, W. *Angew. Chem., Int. Ed. Engl.* **1984**, *23*, 272.

JP900735W